Electronic Supplementary Information

High capacity and exceptional cycling stability of ternary metal sulfide nanorods as Li ion battery anode

Dhrubajyoti Bhattacharjya,[a,b] Apurba Sinhamahapatr[a] Jae-jung Ko,[b] and Jong-Sung Yu[a,*]

[a]Department of Energy Systems Engineering, Daegu Gyeongbuk Institute of Science and Technology (DGIST), Daegu, 711-873, Republic of Korea. E-mail: jsyu@dgist.ac.kr; Tel.: (+82) 53-785-6443, Fax: (+82) 53-785-6409

[b]Department of Advanced Materials Chemistry, Korea University, 2511 Sejong-ro, Sejong 339-700, Republic of Korea.

Materials

Cobalt acetate tetrahydrate ($Co(OAc)_2 \cdot 4H_2O$), nickel acetate tetrahydrate ($Ni(OAc)_2 \cdot 4H_2O$), thiourea ($(NH_2)_2CS$), ethylene glycol (EG), sodium carboxymethyl cellulose (CMC) and water soluble polyacrylamide (PAA) were commercially available from Sigma Aldrich in analytical grade and were used without further purification. Deionized water with an electrical resistance of 18 MΩ is used throughout.

Synthesis of $NiCo_2S_4$ nanorods

In a typical synthesis of $NiCo_2S_4$ nanorods, $Ni(OAc)_2 \cdot 4H_2O$ (0.15 mmol), $Co(OAc)_2 \cdot 4H_2O$ (0.3 mmol) and thiourea (0.9 mmol) were dissolved in 60 mL of water/EG (1:1, v/v) mixed solvent and stirred at room temperature for 1 h to get a clear solution. Then, the clear solution was transferred to a teflon lined stainless-steel autoclave (80 mL) and heated at 160 °C for 24 h. After cooling to room temperature naturally, the resulted product was collected by filtration, washed with plenty of deionized water and ethanol to remove any residual impurities and then dried at 80 °C for 12 h to get $NiCo_2S_4$ nanorods. Co^{2+} is converted to Co^{3+} during the hydrothermal process. The synthesized product was pyrolysed at 300 °C in inert atmosphere for 2 h to increase the crystallinity of the final $NiCo_2S_4$ nanorods.

Physical characterization

The morphology of all the synthesized $NiCo_2S_4$ nanorods was observed on Hitachi scanning electron microscope (SEM) S-4700 that operated at an acceleration voltage of 10 kV and on high resolution transmission electron microscopy (HR-TEM) JEOL FE-2010 operated at 200 kV. X-ray diffraction (XRD) data were obtained using a Rigaku Smartlab diffractometer with Cu-Ka (0.15406 nm) operated at 40 kV and 30 mA at a scan rate of 2° min^{-1}. X-ray photoelectron

spectroscopy (XPS) was performed to analyse surface elemental compositions of $NiCo_2S_4$ nanorods using an ESCALAB 250 XPS System with a monochromated Al Ka (150 W) source.

Electrode preparation

The sample of $NiCo_2S_4$ nanorods, conductive carbon (Super P, Timcal) and mixed binder (2:1 w/w ratio of CMC and PAA) was mixed together with a weight ratio of 70:15:15 using water as solvent, and then the resultant uniform slurry was casted on the copper foil by the doctor blade to make a 20 μm thin film. The prepared thin film was kept for drying initially at room temperature overnight and then at 80 °C in vacuum oven overnight. This thin film was then pressed by the rolling machine before punching to the circular electrode with a diameter of 14 mm (Ø14). Approximately 1.5-2.0 mg of active material was loaded in each electrode. For comparison, $NiCo_2S_4$ nanorod electrodes were also prepared by the same process except using only polyvinylidene difluoride (PVDF) as binder and 1-methyl-pyrrolidone as solvent keeping all other parameters and process unchanged.

Cell construction and electrochemical performance measurement

To test the electrochemical performance of the $NiCo_2S_4$ nanorod anodes, the coin cells were assembled in an argon-filled glove box (H_2O, O_2 < 0.1 ppm) using CR 2032 coin cell (Hohsen Corp., Japan) with lithium metal (purity, 99.9% and 150 mm thick) as a counter and reference electrode and Celgard 2400 as a separator. The electrolyte used was 1.0 M $LiPF_6$ dissolved in a mixture of ethylene carbonate (EC) and dimethyl carbonate (DMC) (1: 1 by volume, Soulbrain Pte. Ltd.). The electrochemical performance of the prepared coin cells was examined by galvanostatic charge–discharge measurement in a BaSyTec multichannel battery test system. The instrument was programmed to read in each 10 s step. The cells were galvanostatically charged-discharged (CD) at the current density of 100 mA g^{-1} in the voltage range of 0.01 - 3.0 V vs. Li/Li^+ at room temperature. Cyclic voltammetry (CV) experiments were carried out using an electrochemical workstation (Biologic VSP-1) in the potential range of 0.01 - 3.0 V at the scan rate of 0.1 mV s^{-1}. Electrochemical impedance spectroscopy (EIS) measurements were carried out in the frequency range of 100 kHz – 100 mHz with an amplitude of superimposed AC signal of 0.01 V.

The charge discharge process in $NiCo_2S_4$ nanorod anodes can be explained through following electrochemical reactions:

First discharge process:

$$NiCo_2S_4 + 8Li + 8e^- \rightarrow Ni + 2Co + 4Li_2S \quad (1)$$

Second and subsequent charge-discharge process:

$$Ni + Li_2S \leftrightarrow NiS + 2Li + 2e^- \quad (2)$$

$$Co + Li_2S \leftrightarrow CoS + 2Li + 2e^- \quad (3)$$

$$Li_2S \leftrightarrow 2Li + S + 2e^- \quad (4)$$

Overall cell reaction:

$$Ni + Co + 3Li_2S \leftrightarrow NiS + CoS + 6Li + S + 6e^-$$

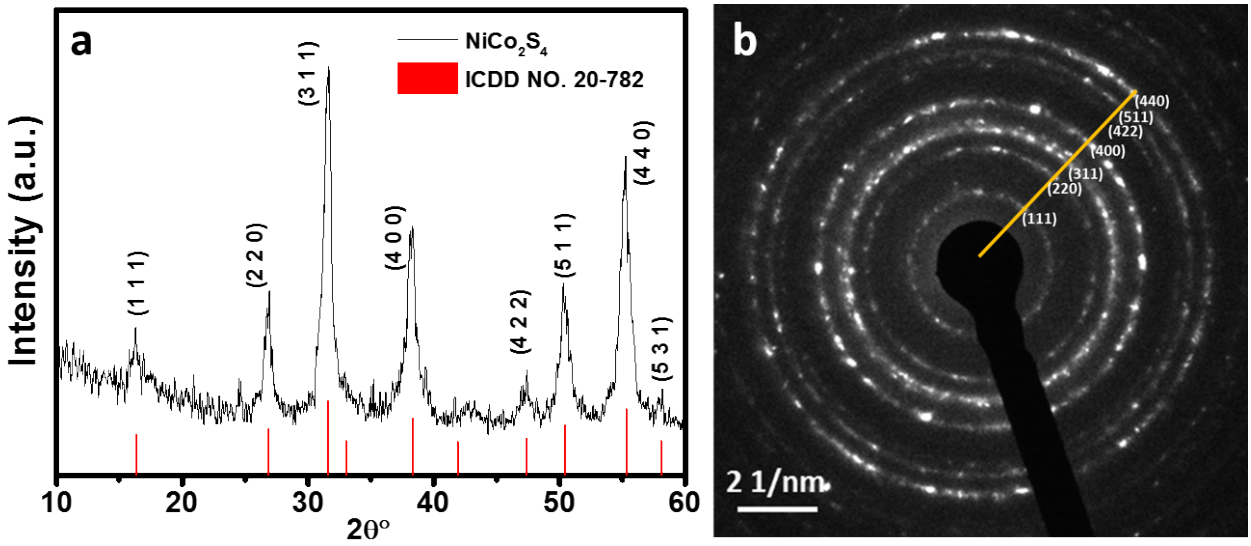

Fig. S1 (a) XRD pattern with ICDD reference peaks and (b) selected area electron diffraction pattern for $NiCo_2S_4$ nanorod sample.

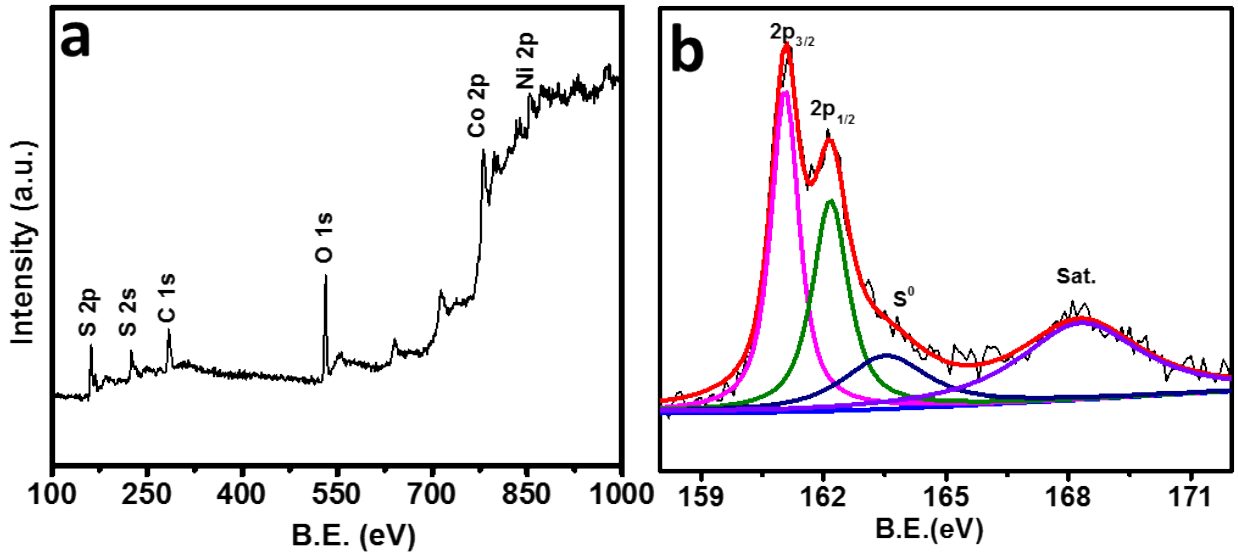

Fig. S2 (a) XPS survey plot and (b) high resolution S 2p spectrum with Gaussian fitting for synthesised $NiCo_2S_4$ nanorod sample.

The presence of C (as reference) and O elements are due to exposure of $NiCo_2S_4$ nanorod samples to moisture and/or air during drying and heating processes.[1-3]

1. Shen, L.; Wang, J.; Xu, G.; Li, H.; Dou, H., Zhang, X., *Adv. Energy Mater.* **2015,** *5,* 1400977.
2. Chen, H.; Jiang, J.; Zhao, Y.; Zhang, L.; Guo, D., Xia, D., *J. Mater. Chem. A* **2015,** *3,* 428.
3. Pu, J.; Cui, F.; Chu, S.; Wang, T.; Sheng, E., Wang, Z., *ACS Sustainable Chem. Eng* **2014,** *2,* 809.

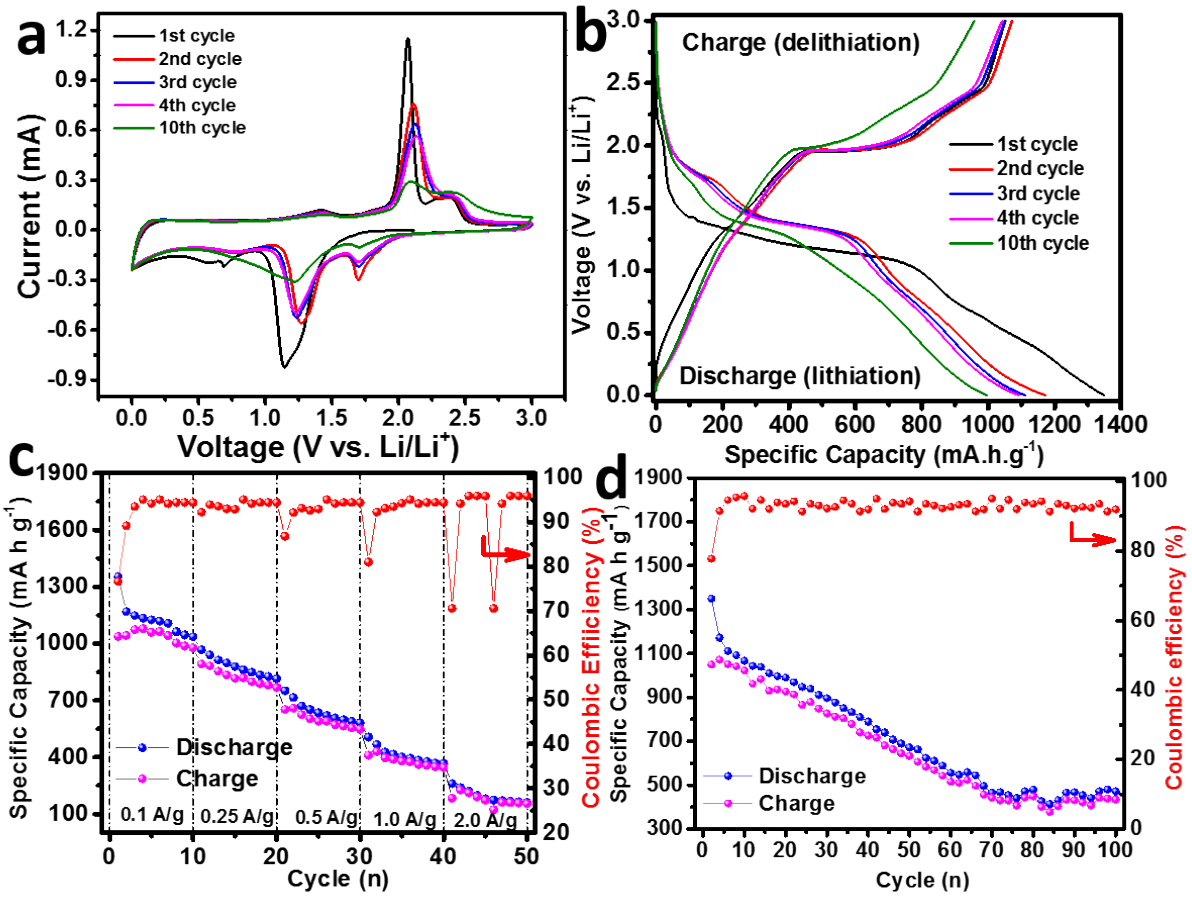

Fig. S3 Electrochemical performance of the $NiCo_2S_4$ nanorod anodes fabricated using PVDF binder: (a) CV curves and (b) CD curves for the initial few cycles, (c) rate performance at different current density, and (d) cycling performance for 100 charge-discharge cycles at 1.0 A g^{-1}.

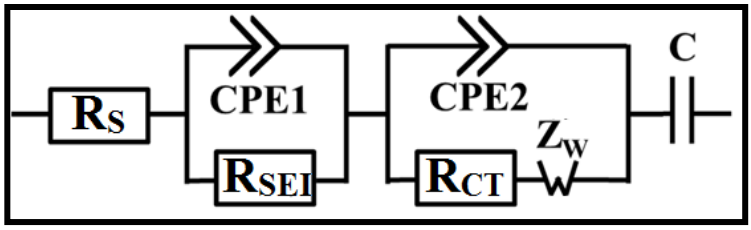

Fig. S4 The equivalent electrical circuit associated with the Li charge-discharge process in $NiCo_2S_4$ anodes.

The starting point of the EIS Nyquist plot at high frequency region is the electrolyte resistance (R_S). This is followed by a depressed semicircle in the high to middle frequency region, which consists of two semicircles with each corresponding to a parallel combination of a constant phase element (CPE) and a resistive element. One resistive element is SEI resistance (R_{SEI}) and the other is charge transfer resistance (R_{CT}). The inclination from semicircle at middle to low frequency region determines the Warburg impedance (Z_W), which determines the resistance for Li ion diffusion through the electrode surface. The straight line at low frequency determines the capacitance (C) at electrode-electrolyte interface. The EIS Nyquist plots after different CV cycles are fitted with the above-shown circuit with the help of ZFit software, and the data are given in Table S1.

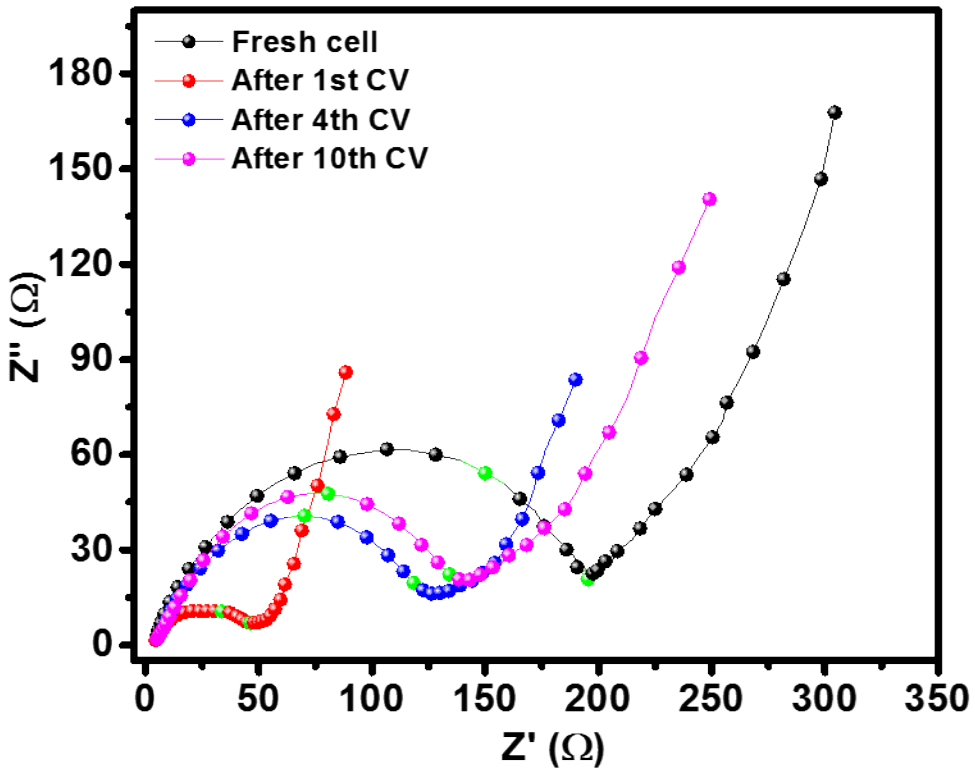

Fig. S5 EIS Nyquist plots for the $NiCo_2S_4$ nanorod anodes fabricated using PVDF binder before and after different CV cycles. (Green coloured points in each Nyquist plot show the data points recorded at 250 Hz and 25 Hz, respectively).

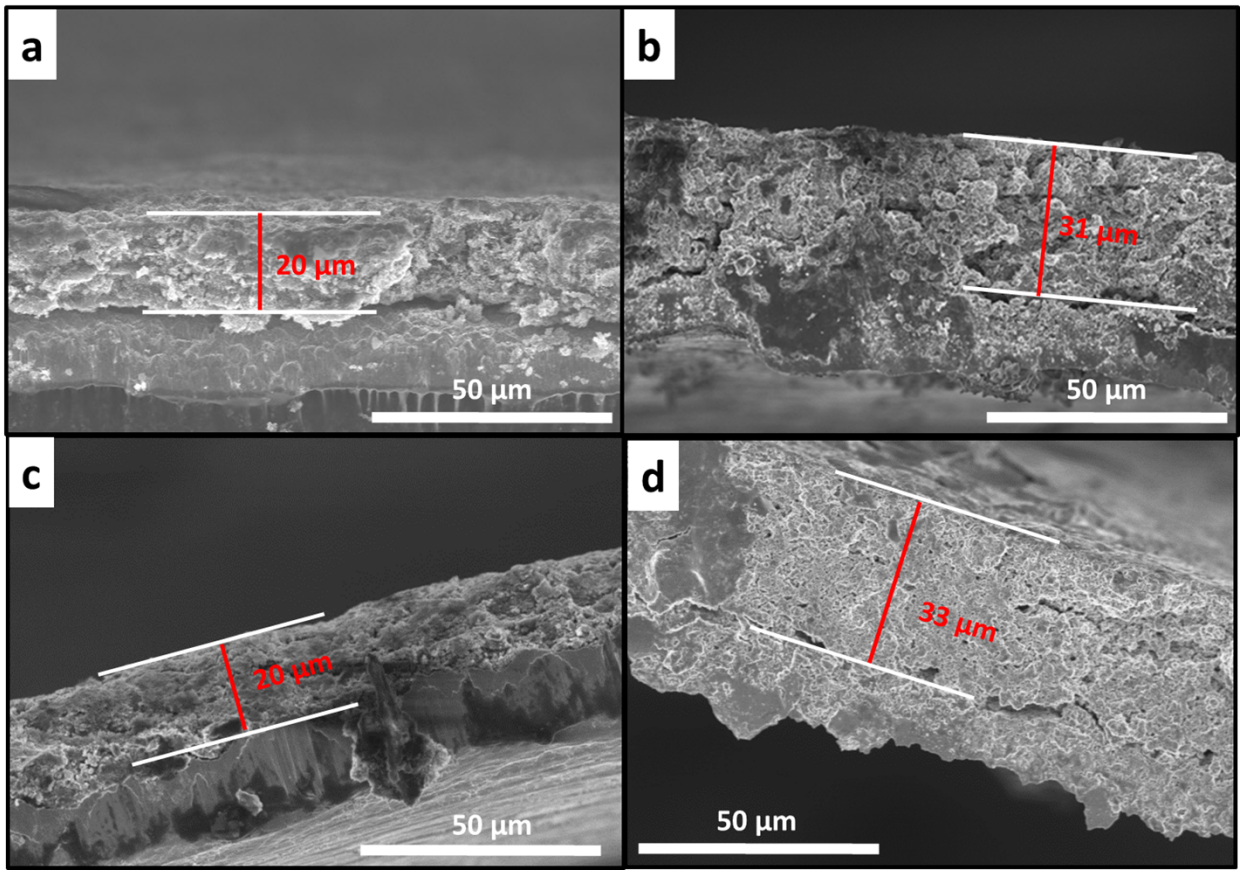

Fig. S6 SEM images for cross section of electrodes showing thickness: (a) fresh electrode with CMC-PAA binder, (b) electrode with CMC-PAA binder after 10 CV cycles, (c) fresh electrode with PVDF binder, and (d) electrode with PVDF binder after 10 CV cycles.

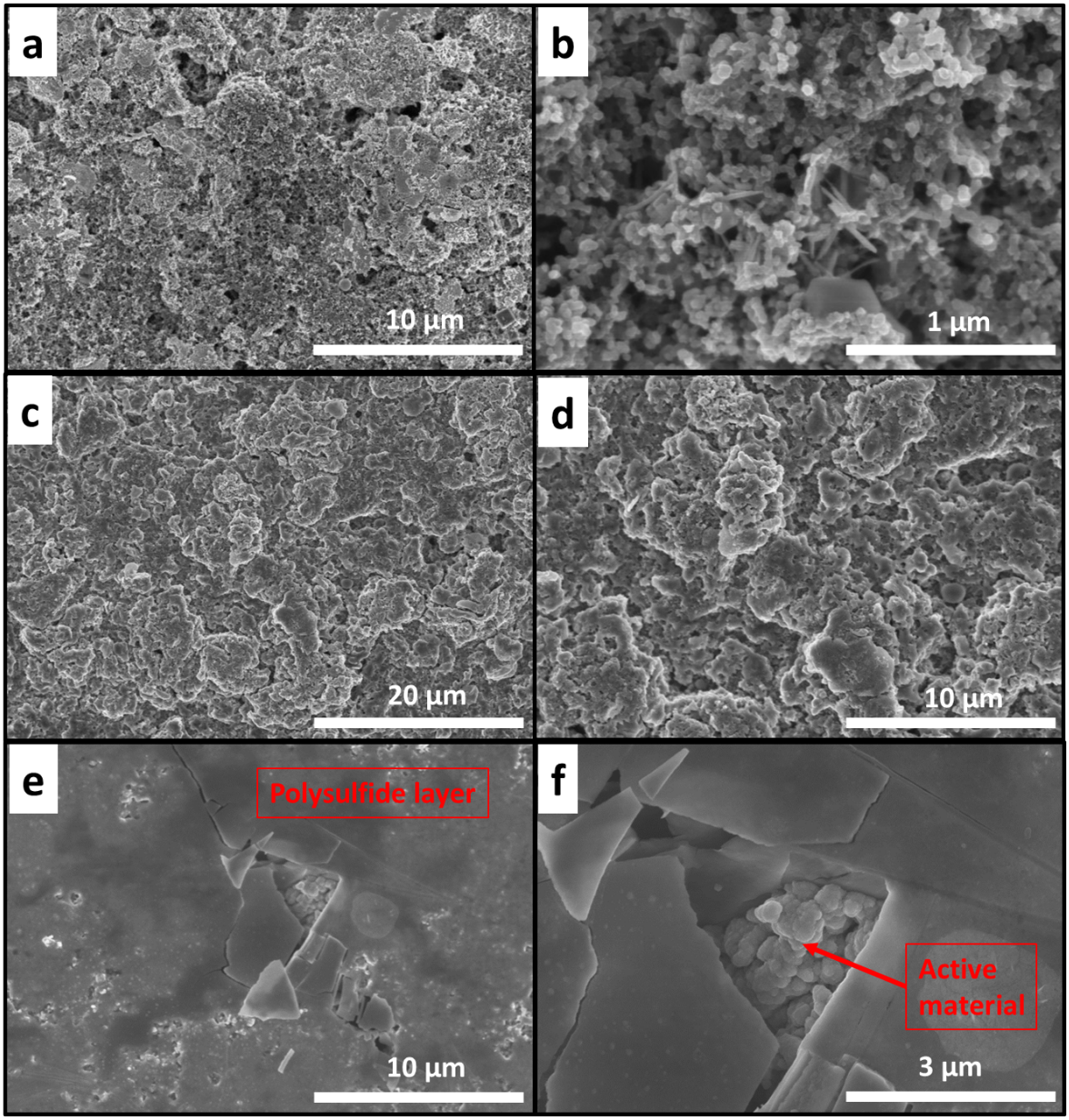

Fig. S7 SEM images of $NiCo_2S_4$ electrodes: (a) low resolution image of fresh electrode, (b) high resolution image of fresh electrode showing the $NiCo_2S_4$ nanorods, (c) and (d) low resolution images of electrode fabricated with CMC-PAA binder after 10 CV cycles showing the rough morphology but no cracks, (e) low resolution image of electrode fabricated with PVDF binder after 10 CV cycles showing the thick polymeric gel layer with some cracks, and (f) high resolution image of a crack showing active materials get trapped below the polymeric gel layer.

Table S1 The impedance parameters for the $NiCo_2S_4$ anodes fabricated with CMC-PAA binder after different electrochemical measurements based on Fig. 3 in the main manuscript

		R_S (Ω)	R_{SEI} (Ω)	R_{CT} (Ω)	Z_W ($\Omega.s^{-1/2}$)
During CV test	After 1st CV	4.2	1.7	19.4	26.7
	After 4th CV	5.1	2.3	9.7	22.9
	After 10th CV	4.6	1.5	6.3	11.8
During rate performance test	After first 10 CD cycles at 0.1 A g^{-1}	12.0	31.1	54.0	22.4
	After 10 CD cycles at 2.0 A g^{-1}	18.6	11.3	24.7	18.9
During cycling stability test	After first 10 CD cycles at 0.1 A g^{-1}	10.0	27.1	31.0	19.6
	After 100 CD cycles at 0.1 A g^{-1}	10.4	14.3	17.4	19.3